Journal of Advanced Research 21 (2020) 91–102

Contents lists available at ScienceDirect

Journal of Advanced Research

journal homepage: www.elsevier.com/locate/jare

Hydroxyapatite/silver electrospun fibers for anti-infection and osteoinduction

Feifei Liu [a,1], Xiaohui Wang [a,1], Tongtong Chen [b], Naiyin Zhang [c], Qin Wei [d], Juling Tian [e], Yingbo Wang [a,*], Chuang Ma [f,*], Yong Lu [b,*]

[a] College of Chemical Engineering, Xinjiang Normal University, Urumqi 830054, Xinjiang, PR China
[b] Radiology Department, Ruijin Hospital, Shanghai Jiao Tong University School of Medicine, 197 Ruijin 2nd Road, Shanghai 200025, PR China
[c] College of Life Information Science and Instrument Engineering, Hangzhou Dianzi University, Xiasha Higher Education Zone, Hangzhou, Zhejiang 310018, PR China
[d] Animal Laboratory Center, Xinjiang Medical University, 393 Xinyi Road, Urumqi 830054, PR China
[e] Laboratory Department of the First People's Hospital of Urumqi, 1 Jiankang Road, Urumqi 830002, PR China
[f] Department of Orthopedics Center, the First Affiliated Hospital of Xinjiang Medical University, 393 Xinyi Road, Urumqi 830054, PR China

HIGHLIGHTS

- Stable silver-nanoparticles coating layer using electrochemical method.
- Dopamine self-polymerized on the surface of electrospun fibers.
- Steady and slow release of Ag for long-term antibacterial property.
- Calcium phosphate surface for bioactivity and osteoinductivity.

GRAPHICAL ABSTRACT

Osteoinductive and persistent antibacterial PLLA/HA/PDA/PPy/Ag composite fiber was successfully synthesized through the self-polymerization of Dopamine on the surface of PLLA/HA and electrochemical deposition of PPy-controlled Ag-NPs.

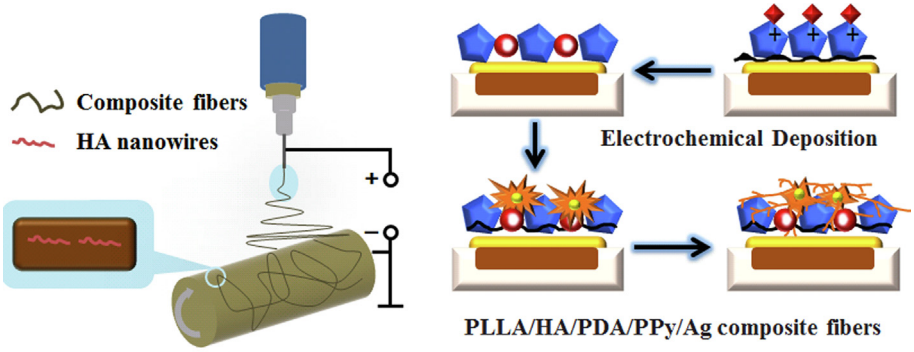

ARTICLE INFO

Article history:
Received 5 August 2019
Revised 19 September 2019
Accepted 6 October 2019
Available online 9 October 2019

Keywords:
Electrospinning
Electrochemical deposition
PLLA
Antibacterial
Osteoinductivity

ABSTRACT

Bone implant materials cause the most common complication of bone infections in orthopedic surgery, resulting in implant failure. Antibiotic treatment of bone infections leads to problems such as bacterial resistance and reduced osteogenic capacity. In this study, dopamine (DA) was self-polymerized on the surface of Polylactic acid (PLLA)/Hydroxyapatite (HA) nanowire composite fibers to form an adhesive polydopamine (PDA) membrane, and a stable silver-nanoparticles (Ag-NPs) coating layer was constructed on it by electrochemically driven Ag^{+} coordination and chelation through Polypyrrole (PPy) mediation, achieving steady and slow release of Ag-NPs. With optimized DA soaking time of 24 h and soaking concentration of 0.5 $g{\cdot}L^{-1}$, nanoparticles were uniformly distributed on PLLA/HA/PDA/PPy/Ag composite fibers and the hydrophilicity of the composite fibers was well-behaved. Besides, the composite fibers possessed good physiological stability and 100% antibacterial rate against *Escherichia coli* (*E. coli*) as well as *Staphylococcus aureus* (*S. aureus*). In addition, the composite fibers had promoted apatite

Peer review under responsibility of Cairo University.
* Corresponding authors.
E-mail addresses: ybwang20002575@163.com (Y. Wang), 8212682@qq.com (C. Ma), 18917762053@163.com (Y. Lu).
[1] These authors contributed equally.

https://doi.org/10.1016/j.jare.2019.10.002
2090-1232/

nucleation and growth on surface and good cytocompatibility with osteoblasts, indicating ability of inducing osteogenic differentiation. In summary, a multi-functional PLLA/HA/PDA/PPy/Ag composite fiber with long-term antibacterial property, bioactivity and osteoinductivity was successfully constructed by electrospinning and electrochemical deposition.

Introduction

Bone tissue infection is the most common complication in orthopedic surgery [1,2], which can damage the self-healing ability of bone tissue, leading to severe bone loss, implant failure and even amputation [3]. In addition, when the self-healing ability of bone tissue is destroyed in the infected region, an artificial matrix that repairs bone could achieve the purpose of bone regeneration. Therefore, the development of biomaterials with dual functions of bone regeneration and infection inhibition has important practical significance for the treatment of bone infection. Polylactic acid (PLLA) is a bioresorbable material with good biocompatibility. It is a clinically recognized biomedical material [4] and plays an important role in guiding bone regeneration [5]. However, PLLA lacks bioactivity, antibacterial ability, and osteoinductivity, which restricts its application in clinical bone repair [6,7]. Nano-hydroxyapatite (n-HA) is a kind of biomaterial that can induce apatite deposition on surface, adhesion and proliferation of cells, and differentiation of bone marrow-derived mesenchymal stem cells (BMSCs). The doping of n-HA can effectively improve the bioactivity and osteoinductivity of PLLA, extending its applications in biomedical field [8,9]. Zhang H et al. prepared PLLA/HA composite as a matrix for bone regeneration, and the results showed that the composite promoted osteogenesis and improved bone regenerative ability [10]. Nevertheless, bone infection problems are often overlooked, leading to implant failure. Bone infections are mainly caused by bacteria [11], and currently, the most common methods of treating bone infections are debridement and systemic antibiotic therapy [12]. Studies have shown that PLLA composite microspheres [13], membranes [14], and porous scaffolds [15], etc., can be used as antibiotic carriers to continuously release antibiotics to treat bone infections. However, long-term and excessive antibiotic treatment may increase the risk of bacterial resistance [16], besides burst problems after antibiotic implantation [17,18]. Therefore, improving the anti-infection ability and reducing the bacterial resistance of PLLA/HA composite fiber has become an urgent need.

From the material science point of view, the nanostructured antibacterial coating on the implant has unique properties such as high specific surface area and surface energy that can mimic the microstructures of natural tissue while possess antibacterial property at the same time [19]. Nano-silver (n-Ag) has a broad spectrum of antibacterial property [20] and minimal bacterial resistance [21], therefore, the introduction of positive n-Ag coating on the surface of PLLA/n-HA composite is an effective way of inhibiting bone infection at early stages. Currently, the methods for constructing n-Ag coating are mainly magnetron sputtering [22] and wet chemical deposition [23]. Magnetron sputtering is a linear technique that cannot be applied to medical materials with complex structures, besides, silver ions (Ag^+) are directly coated on the surface of the material by this method that can cause burst release of Ag^+ at early stages, unable to achieve a long-lasting antibacterial effect. The study of Mishra SK et al. [24] has shown that slow release of Ag^+ is the key to imparting antibacterial effects to coatings in the early stages of tissue implant that usually has high bacterial infection rates. While for the wet chemical deposition method, a discontinuous n-Ag coating can be formed on the surface of PLLA fiber if the deposition time is short. Therefore, it is urgent to construct a uniformly distributed and strongly-bond nano-coating that possesses anti-infection property on the surface of PLLA/HA composite.

Another method, electrochemical deposition, is a non-linear technique that can enhance the adhesion between the substrate and the coating [25]. In addition, it has the functionality to prepare uniform coatings on complex surfaces and control the morphology of the coating precisely by adjusting the electrochemical parameters. However, n-Ag exhibits a high electrodeposition rate, leading to strong tendency of n-Ag agglomeration [26] and affect cell viability. The generally used electrochemical method for regulating particle uniformity is adding regulator to the electrolyte. Polypyrrole (PPy) is a conductive and biocompatible polymer that can be prepared by electrochemical method to assist in the deposition and slow release of n-Ag. Polypyrrole-nanoparticles (PPy-NPs) can be obtained by addition polymerization of α and β positions of pyrrole monomer (Py) under electrochemical oxidation [27]. There are amine groups present in PPy molecules so PPy is widely used in adsorbing metal ions such as Cr^{4+} [28], Co^{3+} [29] and Ag^+ [30], indicating the capability of PPy acting as a stabilizer for n-Ag to prevent its agglomeration. Hnida K E et al. [31] prepared PPy-Ag nanowires on alumina stencil by electrodeposition, and Ag was uniformly dispersed in the polymer matrix under the action of PPy. Xie C et al. [32] prepared a HA/Ag composite coating with good antibacterial property and cell viability by electrodeposition using PPy as a regulator. The above researches have demonstrated that PPy has the unique function of regulating uniform distribution of molecules. However, current researches are all based on the chelation of PPy amine groups with metal ions, which has the problem of poor adhesion between the coating and the substrate [33]. Marine mussels are able to adhere to any material surface through its secreted mucin, while polydopamine (PDA) is a small molecule that mimics the adhesion composition of marine mussels. PDA contains the chemical structure of catechol [34] and exhibits strong adhesion property that makes it be widely used for surface modification of substrates to improve the adhesion of the coatings.

Therefore, in this study, dopamine (DA) was self-polymerized on the surface of PLLA/HA nanowire composite fibers to form an adhesive PDA membrane, and then electrochemical deposition was performed with PPy-regulated Ag^+ coordination and chelation to construct a stable slow release n-Ag coating for anti-infection and osteoinduction. Briefly, PDA was formed on the surface of PLLA/HA through self-polymerization of DA. PDA could interact with PPy through hydrogen bond and π-π bond interaction [35], enhancing the surface adhesiveness of PPy composite fiber, preventing the coating from falling off. Then PPy was electrochemically deposited through the coordination and chelation with Ag^+ to form a chelate, allowing Ag^+ movement to the working electrode at a moderate speed. Besides, the strong electrostatic repulsion between PPy molecules has prevented the agglomeration of silver- nanoparticles (Ag-NPs), achieving stable and slow release of Ag-NPs for long-lasting antibacterial purposes. Finally, a versatile fiber with bioactivity, osteoinductivity and antibacterial properties was constructed (Scheme 1).

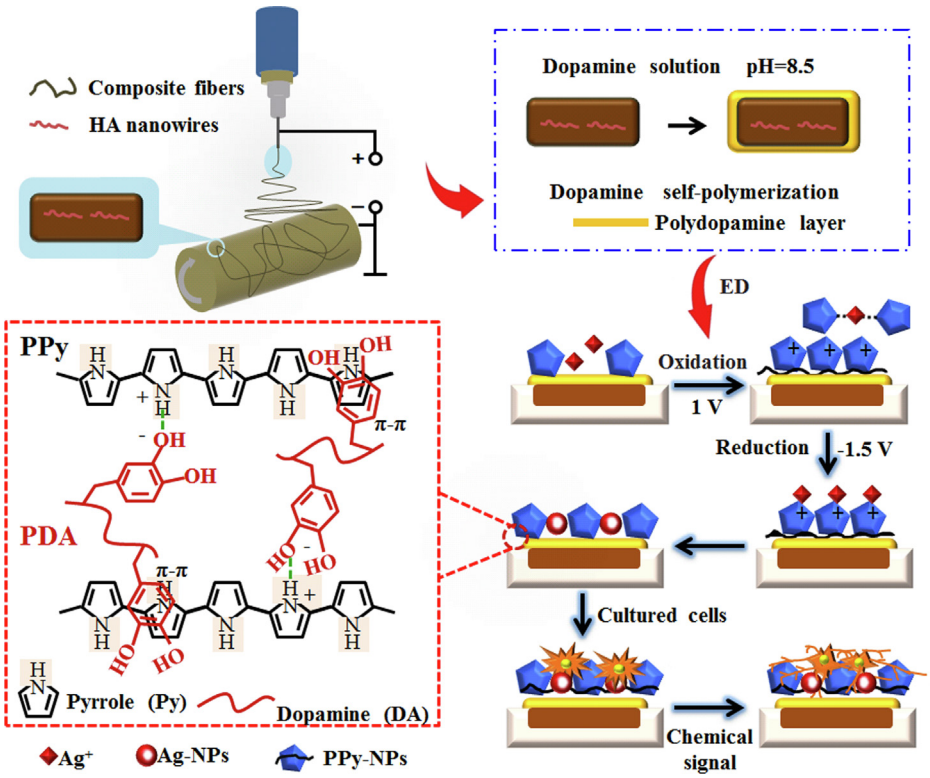

Scheme 1. Synthesis mechanism of osteoinductive PLLA/HA/PDA/PPy/Ag composite fibers for bone infection inhibition.

Materials and methods

Materials and instruments

Polylactic acid (PLLA) was purchased from Jinan Daigang Biomaterial Co., Ltd., China, Mw(PLLA) = 100 kDa. Hydroxyapatite (HA) nanowire was from Suruiyunduan New Material Co., Ltd., China, the average length was 209 nm and the average diameter was 64 nm (Figs. S1 and S3). Trifluoroethanol (TFE) was from Sigma-Aldrich, US. Gelatin (Gel) was from Beijing Chemical Plant, China, Mw (gel) = 50–100 kDa. TL01 Electrospinning Machine was from Shenzhen Tongli Micro-Nano Technology Co., Ltd., China. Scanning electron microscope (SEM, LEO-1430VP) was from Carl Zeiss, Germany. Transmission electron microscope (TEM, JEM-2100F) was from JEOL, Japan. Universal mechanical test instrument (UTM6104) was from Shenzhen Suns Technology Co., Ltd., China. Water contact angle analysis instrument (SDC-200) was from Dongguan Sindin Precision Instrument Co., Ltd., China. Thermogravimetric analysis instrument (STA 449F3) was from NETZSCH, Germany. Confocal microscope (ECLIPSE Ti) was from Nikon, Japan and microplate reader was from Thermo Fisher Scientific, US. Atomic absorption spectrophotometer (AAS, Z-2000, Japan).

Preparation of PLLA/HA composite fiber

To prepare the electrospinning solution for PLLA/HA nanowire composite fiber (PLLA/HA), 0.16 g of gelatin (Gel) was dissolved in 9 mL of Trifluoroethanol (TFE) solution, and HA nanowires was added, followed by sonication for 20 to 30 min. Then 1.44 g of PLLA was added to the solution and stirred for 1 h, configured into an HA nanowire-containing electrospinning solution with PLLA/Gel weight ratio of 90/10. The electrospinning solution was placed into a 20 mL plastic syringe equipped with a medical-grade 6# stainless steel needle. The precursor suspension was adjusted using a syringe pump, and a high voltage of 18 kV·cm^{-1} was supplied through a high-voltage DC power source at a sampling rate of 3 mL·h^{-1}. Electrospinning fibers were collected on an aluminum foil-coated rotating mandrel (20 cm × 13 cm × 0.02 mm) placed 15 cm away from the needle.

Preparation of PLLA/HA/PDA/PPy/Ag composite fiber

The prepared PLLA/HA was cut into squares of 2 cm × 2 cm, and PDA was dip coated on the surface of PLLA/HA. To achieve this, 50 mL of 10 mM Tris (hydroxymethyl) aminomethane (Tris) solution was prepared and the pH was adjusted to 8.5. DA weighing 0.025 g was dissolved in Tris solution to make DA concentration of 0.5 g·L^{-1}, and PLLA/HA was soaked in DA solution for 24 h at room temperature, rinsed with deionized water, and prepared into PLLA/HA nanowire/PDA composite fiber (PLLA/HA/PDA). An electrolyte solution was prepared for electrochemical deposition. Briefly, 0.05 g of $AgNO_3$ and 2 mL of Py were dissolved in 1 L of distilled water to make an electrolyte solution with Ag^+ concentration of 0.05 g·L^{-1} and Py concentration of 2 mL·L^{-1}, and the pH was adjusted to 5.0 with acetic acid. To perform the electrochemical deposition, the 2 cm × 2 cm PLLA/HA/PDA was used as cathode, platinum was anode, and saturated calomel electrode was used as the reference electrode. Samples were placed in a three-electrode electrolytic cell with a conduction time of 2 h and a pulse width of 100 s at room temperature to prepare PLLA/HA/PDA/PPy/Ag composite fiber.

Contact angle and surface energy test

The water contact angle was obtained by differential ellipse fitting. The surface free energy was calculated using the Fowkes equation, also known as the "one-liquid method", which is one of the most commonly used surface energy calculation methods in industry. The reported contact angle was the average of 12 measurements.

Bioactivity test

The samples were cut into squares of 20 mm × 20 mm, weighed and placed in 37 °C, 40 mL, twice the simulated body fluid (SBF) for mineralization (n = 3 for each experimental group). The ingredient of SBF is shown in Table S1, and SBF was replaced every 24 h. Samples were taken out at different mineralization time points (1, 3, 5, 7, 10 days) and soaked in 400 mL of deionized water overnight to remove soluble inorganic ions. After drying at room temperature for 72 h, samples were weighed again and spray coated with gold to increase surface conductivity, and the morphology of the composite fiber after mineralization was observed with a SEM. The mineralization quantity of apatite on the fiber surface was represented by the increase of fiber mass after mineralization.

Ion release test

The composite fibers were soaked in 40 mL of phosphate buffered saline (PBS, pH = 7.4) for 10 days at 37 °C to investigate the release profile of Ag^+. The absorbance of the leachate (Table S2) was measured by AAS and the concentration of Ag^+ in the leachate was calculated from its standard curve. The physiological stability of the composite fibers was determined accordingly.

Antibacterial property test

The strains used for antibacterial test were *Escherichia coli* (*E. coli*) and *Staphylococcus aureus* (*S. aureus*). Both strains were tested in four experimental groups, including PLLA/HA, PLLA/HA/Ag, PLLA/HA/PPy/Ag, and PLLA/HA/PDA/PPy/Ag (n = 3 for each experimental group).

For the qualitative analysis, stains of *E. coli* and *S. aureus* were inoculated on MH medium separately for activation culture. Then appropriate amount of each strain was acquired and placed in physiological saline to prepare 10 mL bacterial suspensions with a concentration of 0.5 McFarland unit (0.5 MCF, 1.5×10^8 cell·mL^{-1}). Suspensions of each strain with volume of 50 μL were taken out, seeded on a plate and cultured at 37 °C in an incubator for 24 h.

For the quantitative analysis, the antibacterial rate of the sample was calculated to indicate the antibacterial properties of the material. Briefly, the strains were inoculated on MH medium and the process was repeated three times to obtain purified colonies. The samples to be tested were placed under ultraviolet light for 1 h to kill bacteria on the sample surfaces before transferred to a glass slide in a Petri dish. In order to prevent the evaporation of the bacterial suspension, sterile water was added to cover the bottom of the Petri dish. Single colony bacteria were scraped off with the inoculating loop, and the bacterial suspension of 0.5 MCF was prepared using physiological saline. 50 μL of the bacterial suspension was dropped onto the surface of the sample, and cultured in a 37 °C incubator for 24 h. Then 20 μL of the remaining bacterial suspension on the surface of the sample was taken out and seeded on a plate, and the number of colonies was counted after 24 h of culture. The antibacterial rate of the sample was calculated to indicate the antibacterial properties of the material. Three parallel experiments were performed to calculate the average antibacterial rate. The calculation method is shown in Eq. (1),

$$Antibacterial\ rate = \frac{CCCG - CCEG}{CCCG} \times 100\% \quad (1)$$

where CCCG is the colony count of the control group and CCEG is the colony count of the experimental group.

In vitro evaluation of osteoblasts

Osteoblasts were harvested from the calvarial bone of newborn (2 ~ 3 days old) Sprague–Dawley rats. All animal experiments were approved by the Institutional Animal Care and Use Committee (IACUC) of the First Affiliated Hospital of Xinjiang Medical University, and all procedures were carried out in accordance with the Guide for the Care and Use of Laboratory Animals.

Animals were divided into 4 experimental groups, including PLLA/HA, PLLA/HA/Ag, PLLA/HA/PPy/Ag, and PLLA/HA/PDA/PPy/Ag (n = 7 for each experimental group). The samples were placed in a culture plate, and osteoblasts were seeded on the surface of the samples at a seeding density of 3.75×10^4 cell·mL^{-1} with 3.0 mL of α-MEM medium added to each well, and cultured at 37 °C in a CO_2 incubator. After 1, 3, 5, and 7 days of culture, the samples were washed with PBS for three times, fixed and dehydrated, dried and coated with gold to observe the morphology of the cells. In addition, at the time point of 1, 3, 5, and 7 days, CCK-8 was used to examine cell proliferation. Briefly, 100 μL of cell suspension was obtained per well (n = 3 per sample), inoculated in a 96-well plate with 10 μL of CCK-8 added to each well, and incubated at 37 °C for 3 h in a CO_2 incubator. The absorbance of each well was obtained by a microplate reader at a wavelength of 450 nm.

Statistical analysis

A One Sample T test (assuming unequal variance) was used for statistical analysis and all data are presented as mean ± standard deviation. The difference between two sets of data is considered statistically significant when $p < 0.05$.

Results and discussions

This paper has investigated the effect of HA nanowire concentration on the morphology of PLLA fibers. When HA nanowire concentration was low (≤20 wt%), the viscosity of the electrospun liquid was so high that the surface tension was greater than that the electric field force could overcome, resulting in uneven fiber thickness (Fig. 1a). When HA nanowire concentration increased to 30 wt%, the surface of the composite fiber was smooth and the diameter distribution was relatively uniform (Fig. 1b). When HA nanowire concentration continued to increase to 40 wt%, the electrospun solution has lower viscosity, smaller surface tension that electric field force could overcome and the jet was easily stretched to obtain a finer composite fiber (Fig. 1c). According to literature report [36], polylactic acid molecules encapsulate the inorganic compound being added, which destroys the crystallization of polylactic acid in the composite fibers to some extent. With the increase of the added quantity of inorganic compounds, the degree of damage proceeds and crystallinity continues to reduce (Fig. S2). Studies have shown that [37,38] decreases in viscosity are always found when crystallinity of the polymer is reduced. The average diameter of the PLLA/HA composite fibers was 221, 308, and 262 nm when HA nanowire concentration was 20 wt%, 30 wt% and 40 wt%, respectively (Fig. 1d). The HA nanowires were less than 20 nm in diameter (Fig. 1e) encapsulated in, and were distributed along the PLLA fibers (Fig. 1f). This was because that during the electrospinning process, the repulsion in the charged solution was greater than surface tension as the electric field force increased. HA nanowires were oriented from random to highly aligned along the jet line, and thus were orderly wrapped in PLLA fibers [39]. In summary, the HA nanowire concentration of 30 wt% is the preferred experimental condition.

Ag-NPs were added to the composite fibers to improve the antibacterial properties of PLLA/HA. PPy molecule has an amine

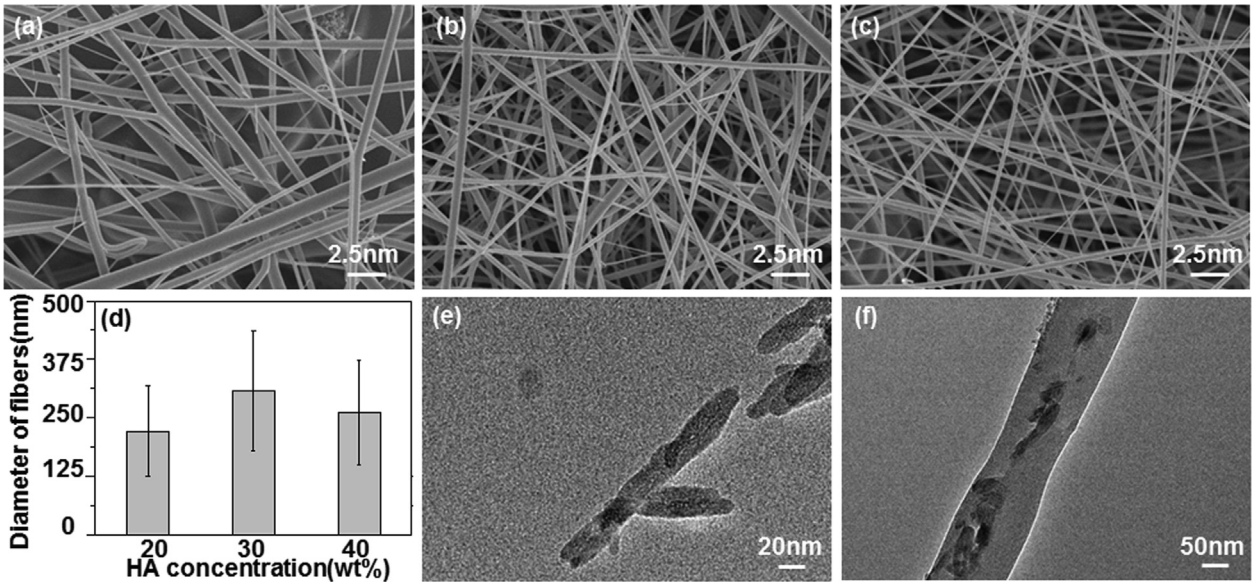

Fig. 1. Characterizations of PLLA/HA with different HA nanowire concentration. SEM micrograph of PLLA/HA with HA nanowire concentration of (a) 20 wt%, (b) 30 wt% and (c) 40 wt%. (d) Average diameter of PLLA/HA fibers. TEM micrograph of (e) HA nanowire and (f) PLLA/HA with HA nanowire concentration of 30 wt%.

group, which is able to adsorb Ag^+ and coordinate with it to form a complex, indicating that PPy can act as a stabilizer for Ag-NPs to prevent its agglomeration. The adhesion efficacy of PPy to the PLLA substrate is relatively low that could not prevent the coating from falling off. In order to improve the adhesion, the bionic macromolecular PDA mimicking mussel adhesion protein was self- polymerized on the surface of PLLA/HA to improve the adhesion between PPy and PLLA fibers. This study has investigated the effect of DA concentration and soaking time on composite fibers.

Effect of DA soaking time on composite fibers

Fig. 2 shows PLLA/HA/PDA/PPy/Ag composite fibers prepared from PLLA/HA with different DA soaking time (12 h, 24 h, 36 h). When PLLA/HA was soaked in DA solution for 12 h, only tiny nanoparticle aggregates were formed on the surface of the fiber (Fig. 2a). When the soaking time increased to 24 h, the size of the nanoparticles increased significantly and nanoparticles were evenly distributed on the composite fiber (Fig. 2b). This phenomenon was due to the expanded self-polymerization time of DA when soaking time increased, during which the composite fiber adsorbed more PPy-Ag, and thereby significantly increased the size of the aggregates. In addition, the sufficient self-polymerization time of DA allowed particle morphology change to nano-spherical form. At the same time, the chelation of Ag^+ with PPy was sufficient to slow down the deposition of Ag-NPs and provide adequate time for crystal growth. Besides, the strong electrostatic repulsion between the PPy molecules prevented the aggregation of Ag-NPs, causing the shape of Ag-NPs to gradually change into a nano-spherical structure, spread uniformly over the entire fiber surface [40]. When the soaking time increased to 36 h, the surface of the composite fiber was completely covered by PDA (Fig. 2c). Since PDA was not conductive, the deposition of PPy was prevented and the shape of particles on the fiber surface became uneven. From the above analysis we could know that the best DA soaking time was 24 h. Besides, the diameter of the nanoparticles on the fiber surface increased as well. This might due to the heterogeneous nucleation processes of PDA aggregates formation [41], during which the deposited PDA acted as heterogeneous nucleation site and inducing more PDA particles to deposit on the fiber surface, adsorbing more PPy-Ag deposits, resulting in significant increase of aggregate diameter. From the above analysis we could know that the number of nucleation sites decreased and the size of deposited DA increased along with time. The uniform distribution of Ag-NPs was critical. It can be seen from Fig. 2d–f that PPy has regulated Ag to be uniformly distributed on the surface of PLLA/HA, and Ag content gradually increased from 0.35% to 0.38% and 1.12% for DA soaking time from 12 h to 24 h and 36 h, respectively (Fig. 2g–i).

Effect of DA concentration on composite fibers

The uniformity of PDA coated on the fiber surface was affected by DA concentration [42]. When DA concentration was 0.0 $g{\cdot}L^{-1}$ ("0.0 $g{\cdot}L^{-1}$" indicated no addition of DA), the fiber surface lacks adhesion to PPy, and only a small amount of Ag-NPs was deposited on it (Fig. 3a). When DA concentration increased to 0.5 $g{\cdot}L^{-1}$, PPy-Ag were uniformly distributed on the surface of the fiber in a nano-spherical shape (Fig. 3b). When DA concentration continued to increase to 1.0 $g{\cdot}L^{-1}$, the surface of the composite fiber was completely covered by PDA (Fig. 3c), and because PDA surface was not conductive, the deposition of PPy was prevented, resulting in uneven sized particle distribution [43]. From the above analysis we could know that the best DA soaking concentration was 0.5 $g{\cdot}L^{-1}$. Ag the element was uniformly distributed on the surface of PLLA/HA (Fig. 3d–f) and DA soaking concentration had a great influence on Ag content. When DA concentration gradually increased from 0.0 $g{\cdot}L^{-1}$ to 0.5 $g{\cdot}L^{-1}$ and 1.0 $g{\cdot}L^{-1}$, Ag content on fiber surface increased from 0.06% to 0.38% and 0.39%, respectively (Fig. 3g–i). It can be seen from the FTIR spectrum (Fig. 3j) of composite fibers with DA concentration of 0.5 $g{\cdot}L^{-1}$, that the C═O stretching vibration peak in PLLA was shown at 1747 cm^{-1}, and the stretching vibration peak of C—O—C in PLLA appeared both at 1076 cm^{-1} and 1179 cm^{-1} [44]. The shearing vibration peak of —NH_2 group in PDA appeared at 1526 cm^{-1} [45] and C═C stretching vibration in PDA benzene ring appeared at 1499 cm^{-1} [46]. The C═C stretching vibration peak of PPy appeared at 1637 cm^{-1} [40], while the bending vibration peak of PO_4^{3-} in HA appeared both at 607 and 567 cm^{-1} [47]. The infrared spectroscopy indicated that PDA was successfully adsorbed on the fiber surface.

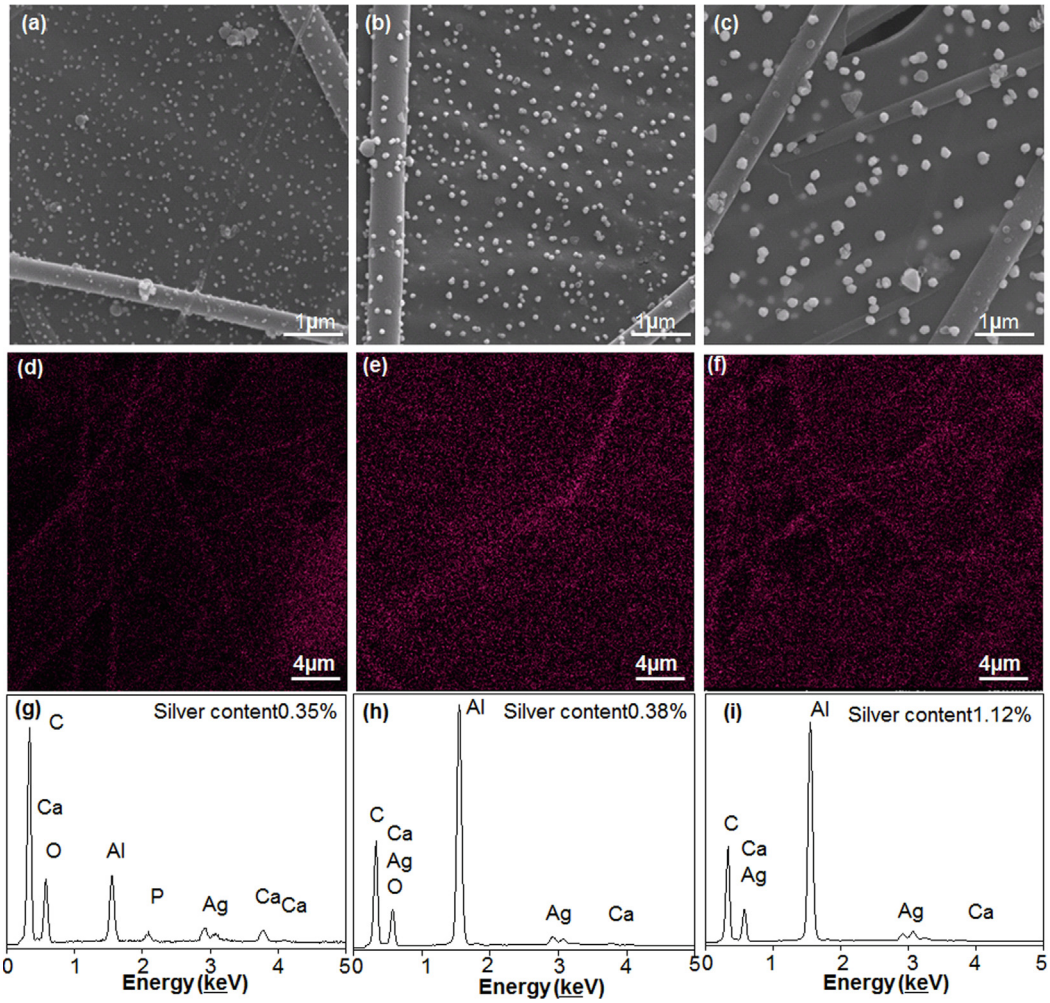

Fig. 2. The influence of DA soaking time on composite fibers. SEM micrograph of composite fibers with DA soaking time of (a)12 h, (b) 24 h and (c) 36 h. Ag distribution on composite fibers after DA soaking for (d) 12 h, (e) 24 h and (f) 36 h. EDS analysis of composite fibers after DA soaking for (g) 12 h, (h) 24 h, and (i) 36 h.

Based on the above analysis, the preferred experimental conditions are 30 wt% HA nanowire, 0.5 g·L^{-1} DA, and 24 h DA soaking time. The hydrophilicity, physiological stability, bioactivity, antibacterial property and cytocompatibility of the composite fiber were analyzed under these conditions.

Analysis of composite fiber properties

Physiological stability and hydrophilicity

Composites used as implant material require high and long-term surface stability in the physiological environment of fluids and activities. Therefore, the physiological stability of the composite fiber was examined in this study. As it can be seen from Fig. 4a, the Ag^+ release rate of PLLA/HA/Ag was 58.4% on day 10 in PBS. When the regulator PPy was added to the fiber, the release rate of Ag^+ significantly reduced to 37.0%. The reason was that PPy was doped as a spherical template in the electrolyte to form Ag-NPs with uniform fiber surface distribution. On the other hand, PPy and Ag^+ were coordinately combined to form PPy-Ag^+ complex, which reduced the release rate of Ag^+. The Ag^+ release rate of the composite fiber with PDA added on the basis of PPy was further reduced to 31.2% because the PDA modification has improved PPy adhesion amount on the surface of the fiber, which decreased the release rate of Ag^+. Therefore, the PLLA/HA/PDA/PPy/Ag composite fibers possess good physiological stability under the dual regulation of PPy coordination and doping, exert long-term antibacterial function and are able to inhibit bone infection.

Surface hydrophilicity is a major factor affecting cellular activities of the composite fibers such as adhesion and migration [48]. Fig. 4b-c showed the hydrophilicity test result of the composite fiber. It can be seen from Fig. 4(b) that PLLA/HA/PDA/PPy/Ag had the lowest contact angle, indicating best hydrophilicity. This was because that the hydrophilic hydroxyl group and amino group presented in PDA had improved the hydrophilicity of the composite fibers [49]. It can be seen from Fig. 4(c) that the surface energy of PLLA/HA/Ag fiber was reduced after adding silver, because silver was easily agglomerated on the fiber surface [50], reducing the surface energy. Polypyrrole can regulate silver, making it less likely to agglomerate and maintain a small size to increase the surface energy. And with the addition of polydopamine, the surface became more hydrophilic and surface energy was increased even more because polydopamine could help polypyrrole regulate the dispersion of silver more uniformly. Therefore, PLLA/HA/ PDA/ PPy/Ag fibers had the highest surface energy and the strongest adsorption capacity.

Antibacterial property of the composite fibers

Bacteria can result in bone infection and reduce the success rate of bone regeneration material implantation [51]. Therefore, the antibacterial properties of biomaterials should be taken into

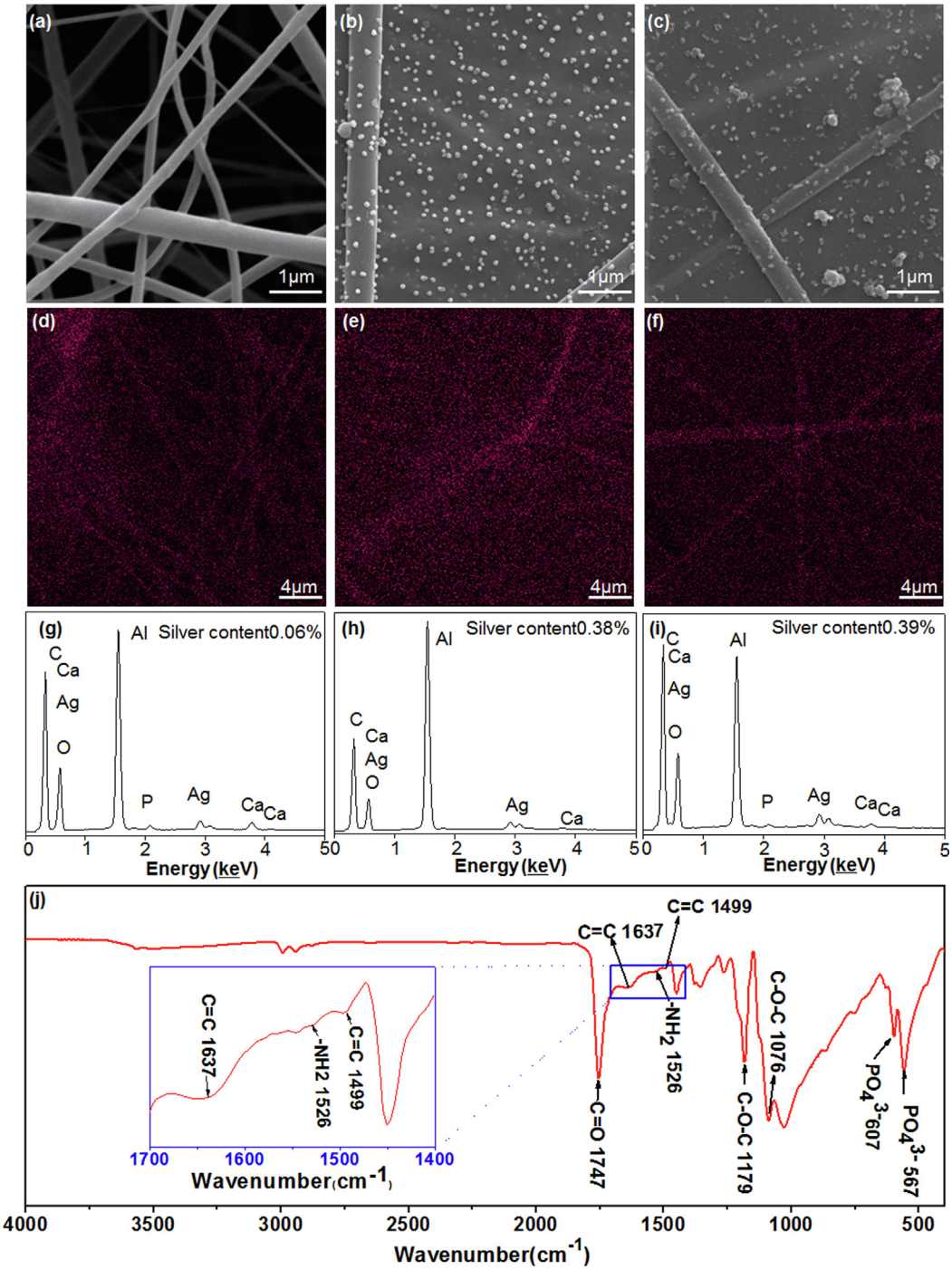

Fig. 3. The influence of DA soaking concentration on composite fibers. SEM micrograph of composite fibers at DA concentration of (a) 0.0 g·L^{-1}, (b) 0.5 g·L^{-1} and (c) 1.0 g·L^{-1}. Ag distribution on composite fibers at DA concentration of (d) 0.0 g·L^{-1}, (e) 0.5 g·L^{-1} and (f) 1.0 g·L^{-1}. EDS analysis of composite fibers at DA concentration of (g) 0.0 g·L^{-1}, (h) 0.5 g·L^{-1} and (i) 1.0 g·L^{-1}. (j) FTIR spectrum of composite fibers with DA concentration of 0.5 g·L^{-1}.

consideration during material development process. *E. coli* and *S. aureus* are not only typical representatives of Gram-positive and Gram-negative bacteria, but also the most common bacteria in clinical infections. In this study, the antibacterial properties of the composites against *E. coli* and *S. aureus* were investigated. It can be seen from Fig. 5a that after 24 h of incubation, the control group of PLLA/HA had no bactericidal ability and bacterial metabolism was active on the fiber surface, forming many *E. coli* and *S. aureus* colonies. Compared to the control group, no *E. coli* colony was found on the surface of PLLA/HA/Ag and PLLA/HA/PPy/Ag, while *S. aureus* colony number was significantly reduced, only showing sporadic *S. aureus* cells. This phenomenon was due to the addition of PPy, which reduced the agglomeration of Ag-NPs, increased its surface area and number of exposed Ag-NPs that could contact with bacteria, and further improved the antibacterial properties of the material. There was no colonies of *E. coli* and *S. aureus* found on the surface of PLLA/HA/PDA/PPy/ Ag, this was because the strong adhesion of PDA could improve the attachment of PPy and Ag-NPs on fiber surface, increasing Ag-NPs content. In the meanwhile, the regulation by PPy reduced the agglomeration

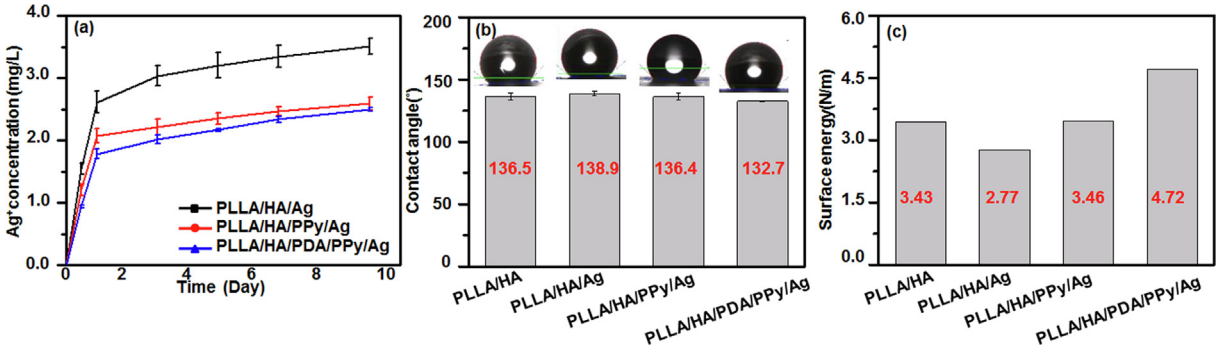

Fig. 4. The (a) Ag^+ release, (b) contact angle and (c) surface energy of the composite fibers.

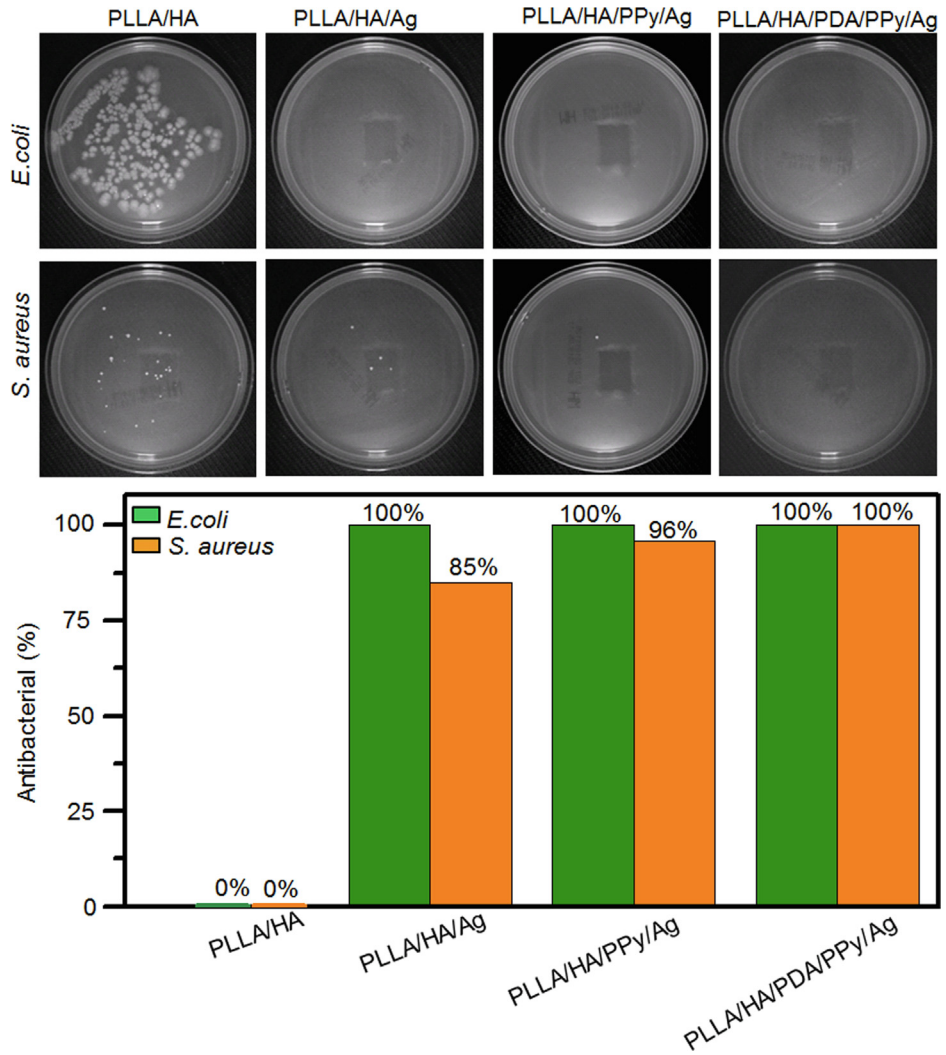

Fig. 5. Antibacterial test result of composite fibers. (a) Qualitative and (b) quantitative analysis of composite fibers against *E. coli* and *S. aureus*.

of Ag-NPs and increased contact area of Ag-NPs with bacteria. Quantitative analysis (Fig. 5b) showed that the antibacterial rates of PLLA/HA/Ag and PLLA/HA/PPy/Ag against *S. aureus* were 85% and 96%, respectively, and both 100% against *E. coli*. While PLLA/HA/PDA/PPy/Ag has antibacterial rate of 100% for both strains. The results showed that PLLA/HA/PDA/PPy/Ag composite fiber has good antibacterial ability against both *E. coli* and *S. aureus*, promising for inhibit bone infections.

Ag-NPs in the composite fiber enhanced its antibacterial property. The cell membrane structures of Gram-positive and Gram-negative bacteria are different, but they are both negatively charged [52]. Therefore, the local Ag^+ that around Ag-NPs in the fiber can raise the bacteria via electrostatic interaction. Meanwhile, the free Ag^+ that released from Ag-NPs can also interact with bacteria [53,54]. Consequently, the local and free Ag^+ synergistically inactivate bacteria enzymes and destroy membrane integrity.

And subsequently, Ag^+ is released from the dead bacteria and can contact with other colonies, and the above process is repeated. Therefore, Ag can maintain a long-lasting antibacterial property. Studies have shown that PDA-modified scaffolds can reduce bacterial binding [55]. Although PLLA/HA/PDA/PPy/Ag composite fiber has excellent antibacterial properties, it does not affect cell adhesion and proliferation. It has been reported that 2.4 wt% of Ag in the composite coating could promote proliferation and differentiation of bone marrow stromal cells with no cytotoxicity [32]. The Ag content in this study was 0.38%, lower than the reported value and PPy has function of chelating with Ag^+ to reduce its toxicity.

Bioactivity of composite fibers

Bioactivity is one of the most important properties for evaluating osteointegration of bone repair materials, and the indicator is the nucleation and growth of bone-like apatite on the surface of the material. In this study, the bioactivity of composite fibers was studied in SBF. It can be seen from Fig. 6a that when the mineralization was conducted for 5 days, only a small amount of apatite was deposited on the surface of each group of fibers, and the deposition quantity was the highest on the surface of PLLA/HA/PDA/PPy/Ag. When the mineralization continued for 10 days, apatite deposition was significantly increased and covered most of the surfaces of the fibers. It can be seen from Fig. 6b that the amount of apatite on the surface of the fiber was proportional to the deposition time and the maximum amount of deposition was reached on day 10. In addition, the deposition increase was significant on day 10 on PLLA/HA/PDA/PPy/Ag fiber surface, which exhibited excellent bioactivity. The high quantity of apatite deposition was due to the good hydrophilicity and great adsorption capacity of PLLA/HA/PDA/PPy/Ag. According to the literature, PDA has the ability to adsorb Ca^{2+}, which is more advantageous to the nucleation and growth of apatite on the fiber surface [56].

In vitro osteogenic evaluation of composite fiber

Fig. 7 shows the SEM micrographs and cell cell activity map of the main functional cell osteoblasts on the surface of each composite fiber after 1, 3, 5, and 7 days of culture. As it can be seen from Fig. 7a, osteoblasts began to adhere on the surface of fibers on day 1 and adhered well on day 3. As cell culture time increased to 5–7 days, osteoblasts showed promoted adhesion and growth, spread well with normal polygonal morphology, and firmly covered the surface of the fibers. Osteoblasts on the surface of PLLA/HA/PDA/PPy/Ag had pseudopods stretched around and increased in number, indicating better osteoblasts adherence. The CCK-8 method was used to detect the proliferation of osteoblasts in the composite fibers (Fig. 7b). On the first day of cell culture, the metabolic activity (OD value) of osteoblasts on the surface of PLLA/HA was the highest. On the third day of cell culture, the metabolic activity of osteoblasts on all groups of composite fibers was similar, and there was no significant difference. On the fifth day of cell culture, the metabolic activity of osteoblasts on the surface of PLLA/HA/PDA/PPy/Ag fibers was the highest. This might be related to the improvement in hydrophilicity of the fiber surface and bioactive functional groups such as —OH and —NH_2. The metabolic activity of osteoblasts on the surface of PLLA/HA/Ag and PLLA/HA/PPy/Ag composite fibers was significantly higher than that of osteoblasts on the surface of PLLA/HA composite fibers. After cultured for 7 days, osteoblasts on PLLA/HA/PDA/PPy/Ag fiber surface possessed the highest metabolic activity while PLLA/HA/Ag

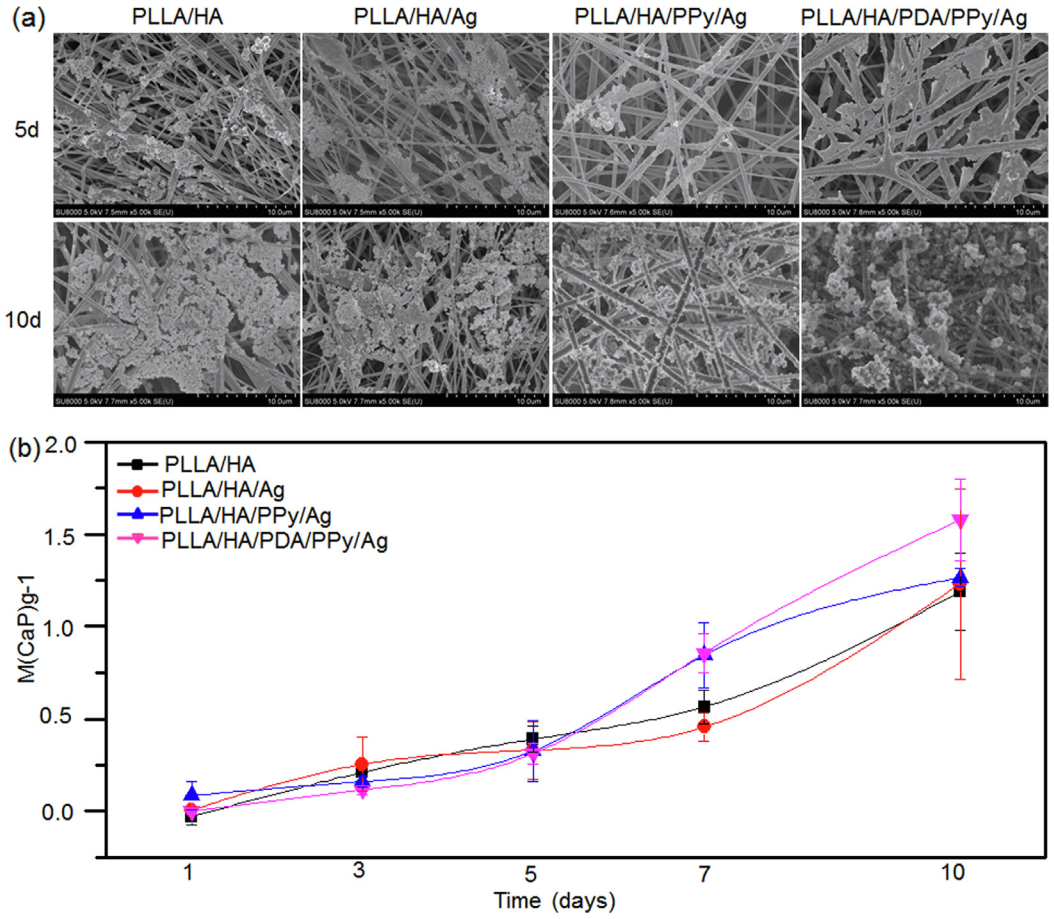

Fig. 6. Mineralization of composite fibers. (a) SEM micrograph of composite fibers after mineralization. (b) Apatite deposition on fiber surface after 1, 3, 5, 7 and 10 days of mineralization.

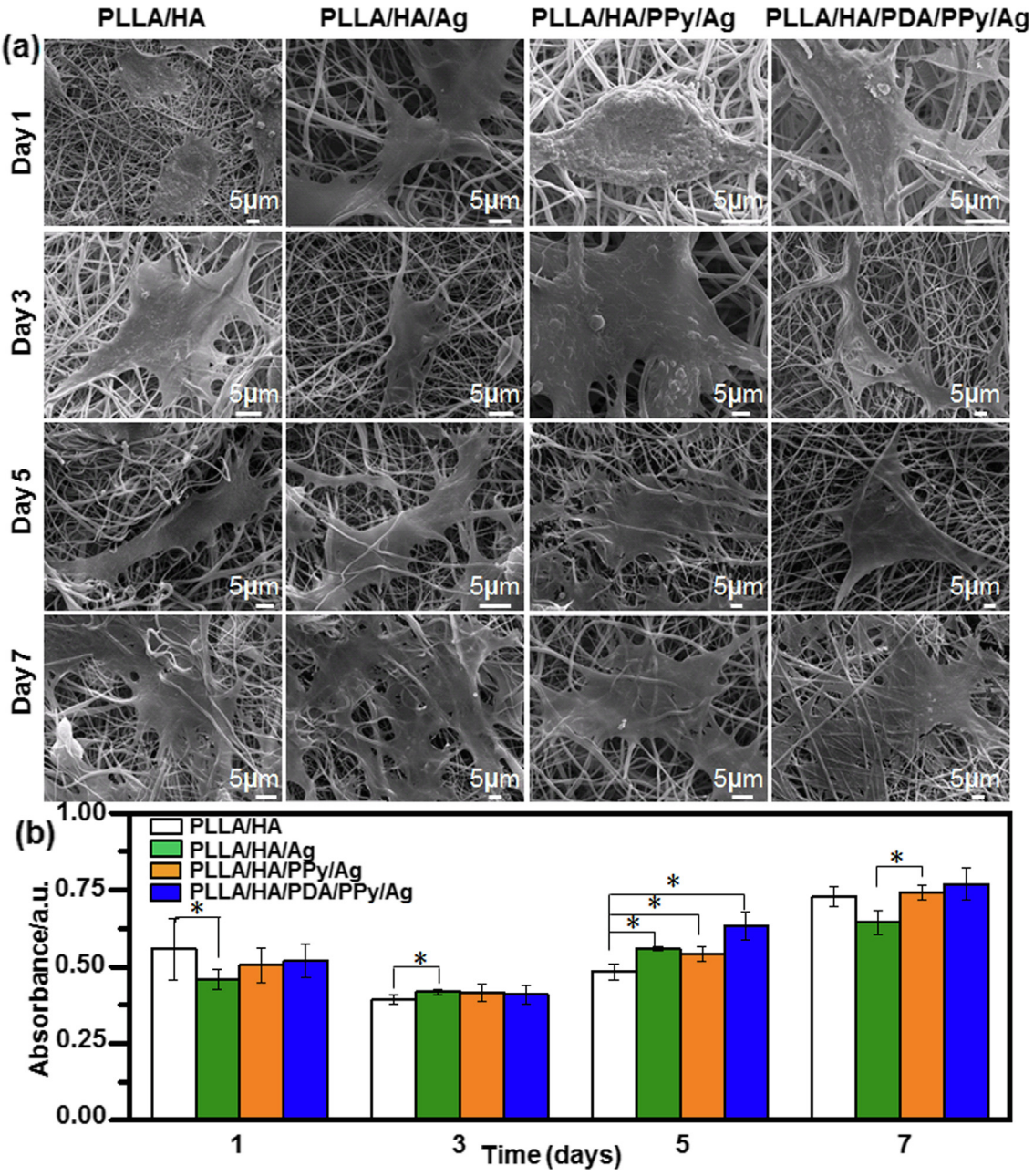

Fig. 7. (a) SEM micrographs and (b) cell activity map of osteoblasts on the surface of each composite fiber after 1, 3, 5, and 7 days of culture.

was the lowest. This result might be due to the local agglomeration of Ag inhibited cell proliferation. In general, the metabolic activity of osteoblasts on the surface of composite fibers increased with the prolongation of culture time. PLLA/HA/PDA/PPy/Ag composite fibers were more favorable for cell proliferation ($p < 0.05$).

Conclusions

Based on the strong adhesion property of PDA, this study has successfully synthesized bioactive, osteoinductive and persistent antibacterial PLLA/HA/PDA/PPy/Ag composite fiber through the self-polymerization of DA on the surface of PLLA/HA and electrochemical deposition of PPy-controlled Ag-NPs. The results showed that along with the increase of DA soaking time and concentration, the diameter of the nanoparticles and silver content of the composite fiber has gradually increased. When DA soaking time was 24 h and soaking concentration was 0.5 $g \cdot L^{-1}$, the nanoparticles were evenly distributed on the fiber surface. Based on the strong affinity of PDA and the dual regulation of PPy coordination and doping, the release rate of Ag^{+} was effectively reduced, which equipped the composite fiber with good physiological stability and long-term antibacterial effect. Moreover, the hydrophilic groups —OH and —NH_2 presented in PDA has enhanced the adsorption capacity and promoted the nucleation and growth of apatite on the surface of the fiber. The antibacterial test results showed that the antibacterial rate of the PLLA/HA/PDA/PPy/Ag composite fiber was as high as 100% against *E. coli* and *S. aureus*. In vitro osteoblast culture showed that the composite fiber has excellent cell compatibility. In this study, a bioactive, osteoinductive and long-term antibacterial PLLA/HA/PDA/ PPy/Ag composite fiber was synthesized by electrospinning and electrochemical deposition, and this material showed promising applications in bone tissue repair for inhibiting bone infection.

Acknowledgments

This work was supported by the National Natural Science Foundation of China (51662038 and, 81560350, 81760397), Outstanding Youth Natural Science Foundation Project of Xinjiang (2017Q002), Research and Innovation Project of Postgraduates in Autonomous Region at 2019. Xinjiang Normal University 2018 College Students Innovative and Entrepreneurship Training Project (201810762007 and 201810762013), Supported by the "13th Five-Year" Plan for Key Discipline Chemistry, Xinjiang Normal University.

Declaration of Competing Interest

We declare that we have no conflicts of interest.

Compliance with ethics requirements

This article does not contain any studies with human or animal subjects.

Appendix A. Supplementary material

Supplementary data to this article can be found online at https://doi.org/10.1016/j.jare.2019.10.002.

References

[1] von Stechow D, Rauschmann MA. Effectiveness of combination use of antibiotic-loaded perossal with spinal surgery in patients with spondylo - discitis. Eur Surg Res 2009;43(3):298–305.
[2] Nandi SK, Mukherjee P, Roy S, Kundu B, De DK, Basu D. Local antibiotic delivery systems for the treatment of osteomyelitis-A review. Mater Sci Eng, C 2009;29 (8):2478–85.
[3] Kolmas J, Krukowski S, Laskus A, Jurkitewicz M. Synthetic hydroxyapatite in pharmaceutical applications. Ceram Int 2016;42(2):2472–87.
[4] Xu X, He L, Zhu B, Li J, Li J. Advances in polymeric materials for dental applications. Polym Chem 2017;8(5):807–23.
[5] Ip WY, Gogolewski S. Clinical application of resorbable polymers in guided bone regeneration. Macromol Symp 2007;253(1):139–46.
[6] Xu T, Yang H, Yang D, Yu ZZ. Polylactic Acid nanofiber scaffold decorated with chitosan islandlike topography for bone tissue engineering. ACS Appl Mater Interfaces 2017;9(25):21094–104.
[7] Ginsac N, Chenal JM, Meille S, Pacard E, Zenati R, Hartmann DJ, et al. Crystallization processes at the surface of polylactic acid-bioactive glass composites during immersion in simulated body fluid. J Biomed Mater Res Part B 2011;99B(2):412–9.
[8] Danoux CB, Barbieri D, Yuan H, de Bruijn JD, van Blitterswijk CA, Habibovic P. In vitro and in vivo bioactivity assessment of a polylactic acid/hydroxyapatite composite for bone regeneration. Biomatter 2014;4(1):e27664–76.
[9] Talal A, McKay IJ, Tanner KE, Hughes FJ. Effects of hydroxyapatite and PDGF concentrations on osteoblast growth in a nanohydroxyapatite-polylactic acid composite for guided tissue regeneration. J Mater Sci: Mater Med 2013;24 (9):2211–21.
[10] Zhang H, Mao X, Du Z, Jiang W, Han X, Zhao D, et al. Three dimensional printed macroporous polylactic acid/hydroxyapatite composite scaffolds for promoting bone formation in a critical-size rat calvarial defect model. Sci Technol Adv Mater 2016;17(1):136–48.
[11] Prasanna APS, Venkatasubbu GD. Sustained release of amoxicillin from hydroxyapatite nanocomposite for bone infections. Prog Biomater 2018;7 (4):289–96.
[12] Penn-Barwell JG, Murray CK, Wenke JC. Early antibiotics and debridement independently reduce infection in an open fracture model. J Bone Joint Surg Br 2012;94B(1):107–12.
[13] Huang YY, Chung TW. Microencapsulation of gentamicin in biodegradable PLA and/or PLA/PEG copolymer. J Microencapsulation 2001;18(4):457–65.
[14] Macha IJ, Ben-Nissan B, Santos J, Cazalbou S, Milthorpe B. Hydroxyapatite/PLA biocomposite thin films for slow drug delivery of antibiotics for the treatment of bone and implant-related infections. Key Eng Mater 2016;696:271–6.
[15] Liu XM, Yang L, Li J, Zhang YM, Xu WJ, Ren Y, et al. GS/DBM/PLA porous composite biomaterial for the treatment of infective femoral condyle defect in rats. Exp Ther Med 2016;11(6):2107–16.
[16] Campoccia D, Montanaro L, Speziale P, Arciola CR. Antibiotic-loaded biomaterials and the risks for the spread of antibiotic resistance following their prophylactic and therapeutic clinical use. Biomaterials 2010;31 (25):6363–77.
[17] Li L, Wang L, Xu Y, Lv L. Preparation of gentamicin-loaded electrospun coating on titanium implants and a study of their properties in vitro. Arch Orthop Trauma Surg 2012;132(6):897–903.
[18] Tu J, Yu M, Lu Y, Cheng K, Weng W, Lin J, et al. Preparation and antibiotic drug release of mineralized collagen coatings on titanium. J Mater Sci Mater Med 2012;23(10):2413–23.
[19] Xiong J, Li Y, Hodgson PD, Wen C. In vitro osteoblast-like cell proliferation on nano-hydroxyapatite coatings with different morphologies on a titanium-niobium shape memory alloy. J Biomed Mater Res A 2010;95A (3):766–73.
[20] Eid KA, Azzazy HM. Sustained broad-spectrum antibacterial effects of nanoliposomes loaded with silver nanoparticles. Nanomedicine (Lond) 2014;9(9):1301–10.
[21] Baker C, Pradhan A, Pakstis L, Pochan DJ, Ismat Shah S. Synthesis and antibacterial properties of silver nanoparticles. J Nanosci Nanotech 2005;5 (2):244–9.
[22] Wang H, Wei Q, Wang X, Gao W, Zhao X. Antibacterial properties of PLA nonwoven medical dressings coated with nanostructured silver. Fiber Polym 2008;9(5):556–60.
[23] Zhang K, Yu HO, Yu KX, Gao Y, Wang M, Li J, et al. A facile approach to constructing efficiently segregated conductive networks in poly(lactic acid)/ silver nanocomposites via silver plating on microfibers for electromagnetic interference shielding. Compos Sci Technol 2018;156:136–43.
[24] Mishra SK, Ferreira JMF, Kannan S. Mechanically stable antimicrobial chitosan–PVA–silver nanocomposite coatings deposited on titanium implants. Carbohydr Polym 2015;121:37–48.
[25] He X, Zhou X, Huang L. Electrodeposition and characterization of Cr-Fe-ZrO_2 composite coating from trivalent chromium chloride electrolyte. Adv Mater Res 2011;239–242:3056–61.
[26] Rezaei B, Damiri S. Electrodeposited silver nanodendrites electrode with strongly enhanced electrocatalytic activity. Talanta 2010;83(1):197–204.
[27] Otero TF. Biomimetic conducting polymers: synthesis, materials, properties, functions, and devices. Polym Rev 2013;53(3):311–51.
[28] Bhaumik M, Setshedi K, Maity A, Onyango MS. Chromium(VI) removal from water using fixed bed column of polypyrrole/Fe_3O_4 nanocomposite. Sep Purif Technol 2013;110:11–9.
[29] Yuasa M, Yamaguchi A, Itsuki H, Tanaka K, Yamamoto M, Oyaizu K. Modifying carbon particles with polypyrrole for adsorption of cobalt ions as electrocatatytic site for oxygen reduction. Chem Mater 2005;17 (17):4278–81.
[30] Wu JJ, Lee HW, You JH, Kau YC, Liu SJ. Adsorption of silver ions on polypyrrole embedded electrospun nanofibrous polyethersulfone membranes. J Colloid Interface Sci 2014;420:145–51.
[31] Hnida KE, Socha RP, Sulka GD. Polypyrrole-silver composite nanowire arrays by cathodic co-deposition and their electrochemical properties. J Phys Chem C 2013;117(38):19382–92.
[32] Xie C, Lu X, Wang K. Pulse electrochemical synthesis of spherical hydroxyapatite and silver nanoparticles mediated by the polymerization of polypyrrole on metallic implants for biomedical applications. Part Part Syst Charact 2015;32(6):630–5.
[33] Kim S, Jang LK, Park HS, Lee JY. Electrochemical deposition of conductive and adhesive polypyrrole-dopamine films. Sci Rep 2016;6:30475–83.
[34] Lee H, Dellatore SM, Miller WM, Messersmith PB. Mussel-inspired surface chemistry for multifunctional coatings. Science 2007;318(5849):426–30.
[35] Xie C, Li P, Han L, Wang Z, Zhou T, Lu X, et al. Electroresponsive and cell-affinitive polydopamine/polypyrrole composite microcapsules with a dual-function of on-demand drug delivery and cell stimulation for electrical therapy. NPG Asia Mater 2017;9:e358–67.
[36] Ma HB, Su WX, Tai ZX, Sun DF, Yan XB, Liu B, et al. Preparation and cytocompatibility of polylactic acid/hydroxyapatite/graphene oxide nanocom po si te fibrous membrane. Chin Sci Bull 2012;57(23):3051–8.
[37] Han S, Wang KK. Shrinkage prediction for slowly-crystallizing thermoplastic polymers in injection molding. Int Polym Proc 1997;12(3):228–37.
[38] Titomanlio G, Speranza V, Brucato V. On the simulation of thermoplastic injection moulding process. Int Polym Proc 1997;12(1):45–53.
[39] Dror Y, Salalha W, Khalfin RL, Cohen Y, Yarin AL, Zussman E. Carbon nanotubes embedded in oriented polymer nanofibers by electrospinning. Langmuir 2003;19(17):7012–20.
[40] Wang Y, Yan L, Cheng R, Muhtar M, Shan X, Xiang Y, et al. Multifunctional HA/ Cu nano-coatings on titanium using PPy coordination and doping via pulse electrochemical polymerization. Biomater Sci 2018;6(3):575–85.
[41] Rim NG, Kim SJ, Shin YM, Jun I, Lim DW, Park JH, et al. Mussel-inspired surface modification of poly (L-lactide) electrospun fibers for modulation of osteogenic differentiation of human mesenchymal stem cells. Colloids Surf B Biointerfaces 2012;91:189–97.
[42] Kim HW, McCloskey BD, Choi TH, Lee C, Kim MJ, Freeman BD, et al. Oxygen concentration control of dopamine-induced high uniformity surface coating chemistry. ACS Appl Mater Interfaces 2013;5(2):233–8.
[43] Popescu S, Ungureanu C, Albu AM, Pirvu C. Poly(dopamine) assisted deposition of adherent PPy film on Ti substrate. Prog Org Coat 2014;77 (11):1890–900.
[44] Gong M, Zhao Q, Dai L, Li Y, Jiang T. Fabrication of polylactic acid/ hydroxyapatite/graphene oxide composite and their thermal stability, hydrophobic and mechanical properties. J Asian Ceram Soc 2018;5(2):160–8.
[45] Bagheri H, Banihashemi S, Zandian FK. Microextraction of antidepressant drugs into syringes packed with a nanocomposite consisting of polydopamine,

silver nanoparticles and polypyrrole. Microchim Acta 2016;183(1):195–202.
[46] Tan J, Zhang Z, He Y, Yue Q, Xie Z, Ji H, et al. Electrochemical synthesis of conductive, superhydrophobic and adhesive polypyrrole-polydopamine nanowires. Synth Met 2017;234:86–94.
[47] Dhand V, Rhee KY, Park SJ. The facile and low temperature synthesis of nanophase hydroxyapatite crystals using wet chemistry. Mater Sci Eng C 2014;36:152–9.
[48] Shamaz BH, Anitha A, Vijayamohan M, Kuttappan S, Nair S, Nair MB. Relevance of fiber integrated gelatin-nanohydroxyapatite composite scaffold for bone tissue regeneration. Nanotechnology 2015;26(40):405101–16.
[49] Ma L, Huang L, Zhang Y, Zhao L, Xin Q, Ye H, et al. Hemocompatible poly (lactic acid) membranes prepared by immobilizing carboxylated graphene oxide via mussel-inspired method for hemodialysis. RSC Adv 2018;8(1):153–61.
[50] Wei T, Yu Q, Chen H. Responsive and synergistic antibacterial coatings: fighting against bacteria in a smart and effective way. Adv Healthcare Mater 2019;8(3):1801381–405.
[51] Huang SH, Chen YJ, Kao CT, Lin CC, Huang TH, Shie MY. Physicochemical properties and biocompatibility of silica doped β-tricalcium phosphate for bone cement. J Dent Sci 2015;10(3):282–90.
[52] Wal AVD, Norde W, Zehnder AJB, Lyklema J. Determination of the total charge in the cell walls of Gram-positive bacteria. Colloids Surf B Biointerfaces 1997;9:81–100.
[53] Su HL, Chou CC, Hung DJ, Lin SH, Pao IC, Lin JH, et al. The disruption of bacterial membrane integrity through ROS generation induced by nanohybrids of silver and clay. Biomaterials 2009;30(30):5979–87.
[54] Hossain Z, Huq F. Studies on the interaction between Ag^{+} and DNA. J Inorg Biochem 2002;91:398–404.
[55] Liu Y, Ai K, Lu L. Polydopamine and its derivative materials: synthesis and promising applications in energy, environmental, and biomedical fields. Chem Rev 2014;114(9):5057–115.
[56] Shen J, Shi D, Shi C, Li X, Chen M. Fabrication of dopamine modified polylactide-poly (ethylene glycol) scaffolds with adjustable properties. J Biomater Sci, Polym Ed 2017;28(17):2006–20.